International Journal of Mechanical and Production Engineering Research and Development (IJMPERD)
ISSN(P): 2249-6890; ISSN(E): 2249-8001
Vol. 6, Issue 3, Jun 2016, 1-10

TRIBOLOGICAL BEHAVIOUR OF WC-Ni CERAMIC COMPOSITES SLIDING AGAINST TUNGSTEN CARBIBE COUNTER FACE

V. CHANDRASEKARAN & D. KANAGARAJAN

Department of Manufacturing Engineering, Annamalai University, Chidambaram, Tamil Nadu, India

ABSTRACT

In this paper, the wear characteristics of Tungsten carbide and Nickel (WC-Ni) composites has been studied for different volume fraction of Tungsten carbide and Nickel-composites with different working conditions to determine the important characteristics like coefficient of friction and wear rate were obtained from the experimental results. The experiments were carried out using a pin-on-roller conFigureuration against a tungsten carbide disk counter face under different sliding speeds, contact load and time. The factor value ranges from 100 to 500 rpm, 10N to 50N and 15min to 75min respectively. The worn out sample and wear debris were examined using scanning electron microscope to reveal the wear features of the test sample of WC/Ni. The test results shows that the wear rates of the composites are gradually reduced over the sliding speed range for both contact loads. Using Minitab software were used to construct the wear maps. The present study focuses to develop wear transition maps and wear mechanism maps for the surface of 5% Ni compositions of WC-Ni composite material. Micro structural characterization results established different dominant mechanisms at different sliding speeds, namely, abrasion, delamination, oxidation, adhesion, thermal softening and melting.

KEYWORDS: Metal Matrix Composite, Tungsten Carbide and Nickel, Wear, Wear Mechanism Map, SEM Observation

Received: Apr 10 2016; **Accepted:** Apr 26 2016; **Published:** Apr 30 2016; **Paper Id.:** IJMPERDJUN20161

Original Article

INTRODUCTION

The combination of Cemented carbide, such as WC−Ni, is generally considered an adequate combination of strength and hardness [1]. This is one of the important reasons for the selection of these materials for a large number of industrial applications, including cutting tools, wear parts, extrusion dies and mining equipment [2].

Engineering materials often lose their effectiveness when it is used for tribological application mainly due to the wear of surface under the combined effect of environment and load. The friction and wear existing in machinery components result in great loss of energy and materials and the energy loss is mainly in the form of the frictional heating. The demand for high-performance materials in modern industry has led to the development of cermet's, such as WC-Ni composites, combining high hardness and high strength with good wear resistance.

Pandey et al [3] has studied the influence of the cemented carbide composition on the tribological application. Various research publications report discussed on influence of the various process parameters on the machining performance of material removal rate (MRR) and surface roughness (Ra) [4-6]. The experimental trials were conducted using the Response surface methodology (RSM) method for the design of the experiments. This method generates the combination of effective processing parameters (as per an orthogonal array) to generate the necessary data with a minimum of experimental trials [7].

A lot of research about Ni3Al taken as alternative binder for cemented carbide has been investigated [8]. This is mainly due to the properties [9] that Ni3Al possess, such as increasing strength with temperature to a maximum at 700−800°C, good oxidation resistance and good resistance to aqueous acidic corrosion environments. At the same time, the wettability of Ni3Al on WC and TiC is sufficient and the possibility of forming compacts of WC/TiC−Ni_3Al has been reported [10]. These properties make Ni3Al a potentially attractive replacement for cobalt in the fabrication of both titanium and tungsten carbide matrix composites [11].

The available research reports describes any grain sizes of the binder material in the tribological behaviour. No literature has been available regarding % composition of matrix and reinforcements. So the present study focuses to develop wear transition maps and wear mechanism maps for the worn out surface of different composition of WC-Ni composite material using MiniTab 16 software.

EXPERIMENTAL STUDY

Specimen Preparation

The available metal powders are of hard tungsten carbides and nickel, which is dry in nature, so the Poly Vinyl Alcohol (PVA) binder is added to obtain a more stable body after pressing. All ingredients are mixed in double cone mixer with alcohol to facilitate the homogenization of the powders. In this research the 150-ton capacity hydraulic press is used for producing green compacts of tungsten carbide and nickel composites. The usual sequence of operations in die compacting include filling of die cavity with a definite volume of 95%WC- 5% Nickel powder, application of the required pressure. The tubular sintering furnace is used for sintering at a temperature of 1250^{o}C for 12hrs to get the required density. Which is carried out at controlled atmosphere for avoiding oxide formation in the surface layers. In this study argon atmosphere is used as sintering medium.

Testing

The wear tests were conducted on a Pin on Roller Friction and Wear testing machine under dry sliding conditions. The test samples were sliding against tungsten carbide disc. The tests was conducted at five different levels of normal force (10 to 50N) sliding speed (100 to 500 rpm) and time (15 to 75min). Therefore total number of experiments conducted for each material is 20. The test specimens were weighed in an electronic weighing balance (CITIZEN CY-360) with an accuracy of 0.001mg prior to testing. The weight loss measurement was taken after running the test in each specimen. During the test, friction force was measured by a transducer mounted on the loading arm thereby coefficient of friction is calculated using the relation $\mu = \frac{H}{F}$, eqn (1) Where H is the frictional force, F is the normal force in Newton. The contact temperature at the counter faces were measured by using thermocouple. Wear rate is calculated by measuring the weight loss of the specimen. WR=Volume of material removed/time in mg/min. The specimens were cleaned thoroughly by using acetone as etchant so as to obtain the clean image of the worn out surface. The different wear mechanisms like ironing, matrix fracture, ploughing, and matrix debonding etc are identified by based on the scanning electron microscope (SEM) observation with the help of the available literature report [12].

RESULTS AND DISCUSSIONS

This study focuses to develop wear transition maps and wear mechanism maps for the surface of 5%Ni compositions of WC-Ni composite material produced through powder metallurgy route. In conventional empirical wear

mechanism maps, it is difficult to establish the boundaries of different mechanisms. Hence it is decided to use Minitab16 software to develop the wear mechanism maps. Table 1 shows the experimental wear test results of WC-5%Ni composites.

Figure 1 shows the coefficient of friction of WC-5%Ni composite, with influence of various sliding speed and contact load. The maximum coefficient of friction 0.75 is obtained at 300rpm of sliding speed with the contact load of 50N and the running time of 45min, and it is minimum 0.13 for the 100rpm sliding speed with 30N contact load and the running time of 45min. And also it seems that the coefficient of friction slightly increases with increase in sliding speed and contact load. This is due to the more plastic deformation takes place at surface asperities rather than elastic deformation.

Table 1: Experimental Results for Wear of WC-5%Ni

Sl. No	Sliding Speed (Rpm)	Contact Load (N)	Time (Sec)	Cof	Wear Rate (Mg/Min)
1	200	40	60	0.21	29.64
2	400	40	60	0.37	43.41
3	200	40	30	0.18	23.66
4	400	40	30	0.64	41.48
5	200	20	60	0.19	15.75
6	300	30	45	0.23	21.24
7	500	30	45	0.52	44.37
8	300	30	45	0.28	22.34
9	300	10	45	0.26	19.12
10	300	30	15	0.36	20.24
11	400	20	60	0.39	37.56
12	300	30	45	0.36	27.49
13	100	30	45	0.13	14.54
14	300	30	45	0.37	23.64
15	300	50	45	0.75	47.24
16	300	30	45	0.32	28.58
17	300	30	45	0.31	27.98
18	300	30	75	0.36	29.76
19	400	20	15	0.32	33.45
20	200	20	15	0.15	16.59

The coefficient of friction is varying with varying the sliding speed, contact load and running time. The average value of coefficient of friction for the 200 rpm with varying contact load of 20 N and 40 N is 0.17 and 0.19 respectively. For the 300rpm sliding speed with different contact load of 10N, 30N and 50N, the coefficient of friction is 0.26, 0.32 and 0.75 respectively. Due to crictical surface energy of the 5% Ni composite, the coefficient of friction increases with increase in contact load [13].

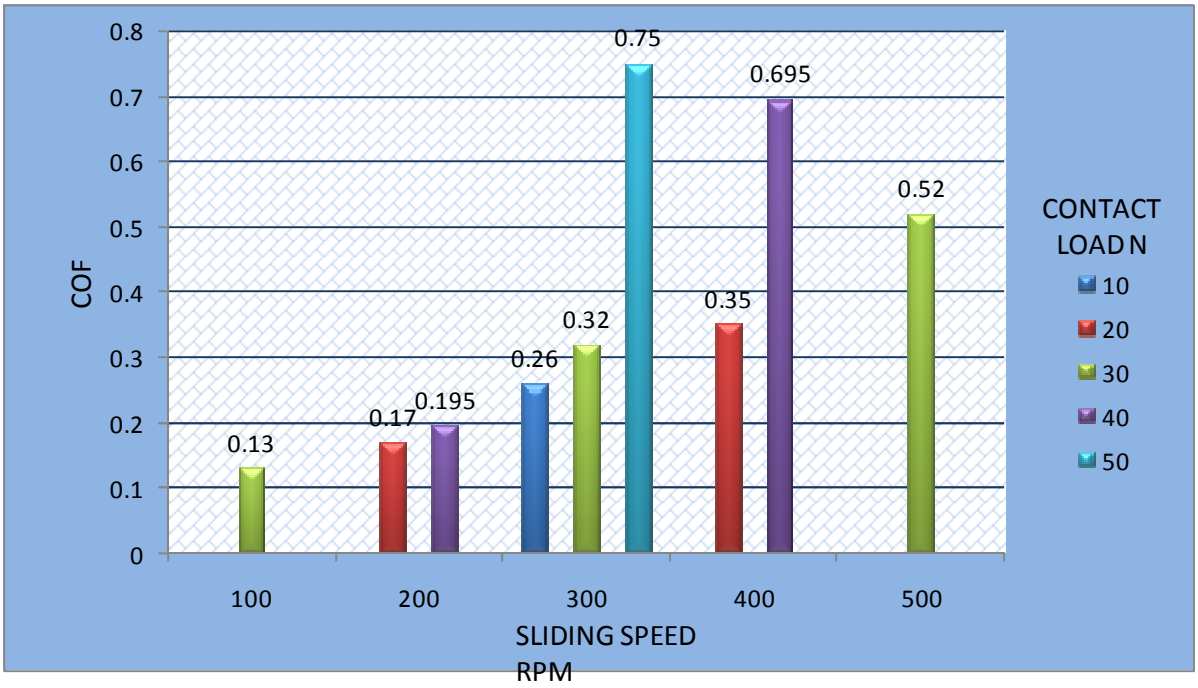

Figure 1: WC-5% Ni Composite COF on Contact Load Vs Sliding Speed

At 400 rpm sliding speed with the different contact load of 20N and 40N, the coefficient of friction was obtained 0.35 and 0.69 respectively. The maximum of sliding speed of 500 rpm with the contact load of 30N and running time of 45min the coefficient of friction obtained 0.52.

Figure 2 shows the specimens are influenced by sliding speed, contact load and running time with the wear rate. The variation of wear rate with the sliding speed of 100, 200, 300, 400, and 500rpm, it is observed that minimum wear rate 14.54mg/min is observed at sliding speed of 100rpm and contact load of 30N and the maximum wear rate 47.24 mg/min is obtained at sliding speed of 500rpm and contact load of 30N. It seems the wear rate increases gradually with contact load.

The wear rate is varying with varying the sliding speed, contact load and running time. The average value of wear rate for the 200 rpm with varying contact load of 20 N and 40 N is 16.17 mg/min and 26.65 mg/min respectively. For the 300rpm sliding speed with different contact load of 10N, 30N and 50N, the average wear rate is 19.12 mg/min, 25.16 mg/min and 47.24 respectively. For 400rpm sliding speed with the different contact load of 20N and 40N, the wear rate was obtained 35.51mg/min and 42.45mg/min respectively. The maximum of sliding speed of 500rpm with the contact load of 30N and running time of 45min the wear rate obtained 44.37mg/min. Also the temperature raised at the surface asperities of contacting surfaces of 5% Ni could deforms and plouging was occurred [14].

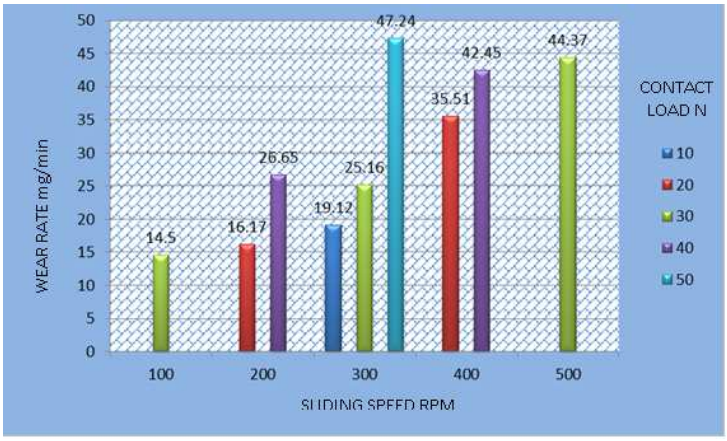

Figure 2: WC-5%Ni composite Wear rate on Contact Load Vs Sliding Speed RPM

At maximum speed and maximum contact load the high temperature was developed between the contact surfaces of the WC-5%Ni composite material. Ni may be melted and debonding from the surfaces. This is known an ploughing mechanisms which is observed at SEM observation of the worn out surfaces.

The WC grains provide high hardness and wear resistance and the nickel binder increases toughness. The question of great practical importance is, how much of the material will be lost during the given operating time. The surface shapes vary due to their functions, manufacturing tolerances, etc. and will be changed as a result of wear and plastic deformation [15].

Wear Mechanism Map

The wear mechanisms of the worn out specimens are studied with help of SEM observations. Hence a wear rate contour map is constructed by keeping melt temperature on X-axis, load on Y-axis and wear rate on Z- axis and it is shown in Figure 3. Williams et al. [12], it is observed that the horizontal contours represents the influences of parameters on X-axis, and the contours in vertical orientation represents the influences of parameters on Y-axis. One of the major problems constructing wear mechanism map is the search of boundries between predominately worn out surfaces that changes the wear rate [16].

By constructing the wear transition map is the search for boundaries of regions of predominant wear and their transitions where the competing processes may change the wear rate. The classification of unlubricated surface interactions involving either mild or severe wear is not based on any particular numerical value of wear rate but rather on observation that increases the severity of the loading conditions (by increasing the force and the sliding velocity) for any pair of materials leads at some stage to a comparatively sudden jump in the wear rate [17]

Wear maps can be constructed systematically by using consistent database, once constructed will provide a material selection guide as well as a design guide for an engineering application. One can also classify the wear processes by using the wear map approach which allows one to conduct critical experiments in the right combination of material, operating condition, and environment to investigate the different wear mechanisms. The classification of boundaries between different wear regimes are not based on any particular numerical value of the wear rate but rather on observation that increased the severity of the loading conditions for any kind of material, which can lead at some stage to a comparatively sudden jump in the wear rate [12].

From an engineering point of view the wear regimes in the wear mechanism map may be classified as mild wear, severe wear and ultra severe wear. The mild wear regimes might be considered as acceptable one, whereas transitions to later regimes are considered as unacceptable. At high sliding speeds, large variations in the slopes of the wear rate curves occurred at a certain load range. The slope changes coincided with the transition from mild wear to severe wear. With help of wear mechanism map a designer can estimate the safest operation condition say sliding speed and contact load, conditions so that any failure can be avoided in the future. The boundaries are classified based on the changes in the orientation of the contour and constructed as wear transition map which is shown in Figure 4a.

Figure 4 shows the wear mechanism map, from this map it is clearly observed that the wear rate ranging from 0 to 0.27mg/min is regarded as mild wear, the wear ranging from 0.27 to 0.51mg/min is considered as severe wear regime and the wear rate exceeds above 0.51mg/min is considered as ultra-sever wear.

The wear rates also increased with the contact load, but there was no drastic increase in the slopes of the wear rate versus load curves, i.e. the mild wear regime prevailed until the higher test load. Severe wear is characterized by massive surface damage and production of large ‘metallic’ debris particles, which are readily identifiable during the test by the naked eye. The onset of severe wear transition to ultra-severe wear has been determined during the course of the wear test by visual observation and the differences in debris types are confirmed by the SEM metallographs.

Figure 4a suggested that surface of the specimen remains polished and shows low volume of wear loss at lower loading conditions of 10N and 20N. The wear mechanism that is identified as more dominant in the mild wear regimes is polishing and scratching, which is obtained for the sliding speed of 100 and 200rpm with the contact load of 10N and 20N. Figure 4b shows the evidence of mostly grooves and ploughing mechanism that are more dominant indicative of micro abrasion being the dominant wear mechanism in the severe wear regimes. These mechanisms are more dominant when the sliding speed of 300rpm with the contact load of 20N and 30N.

Figure 4c shows the evidence of micro fracture and brittle fracture [18]. Brittle fracture has become the dominant wear mechanism in ultra sever wear regimes. The results suggest that significant wear increases as well as change in wear mechanism are associated with this wear transitions. Inter granular fracture is caused by the propagation of these micro cracks, which may be enhanced by the tensile stress induced by friction [19]. For cases of severe abrasive wear involving the coarse abrasives, the mechanism of wear is associated with near surface fractures, initiated primarily from grain boundaries, which caused inter granular cracking and grain pullout [20].

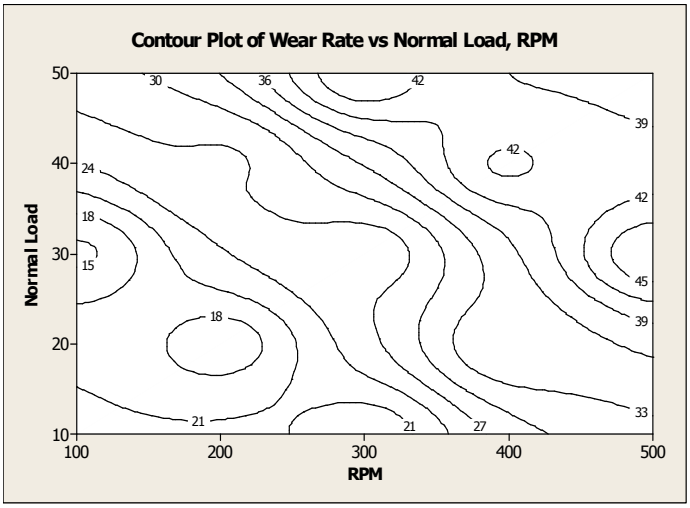

Figure 3: Wear Rate Map for WC-5% Ni Composite

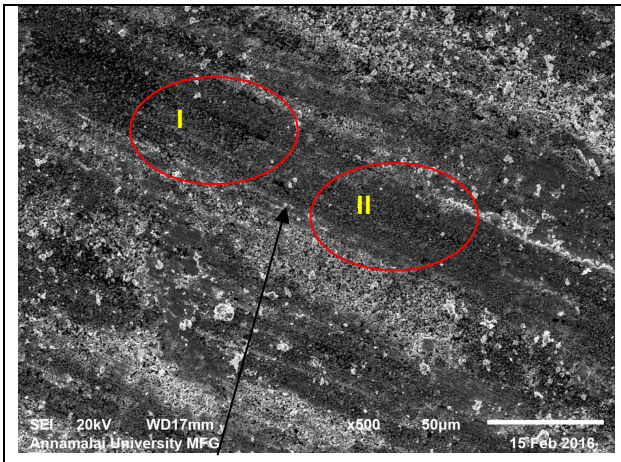

Figure 4a: 5%Ni composite of 20N Contact Load

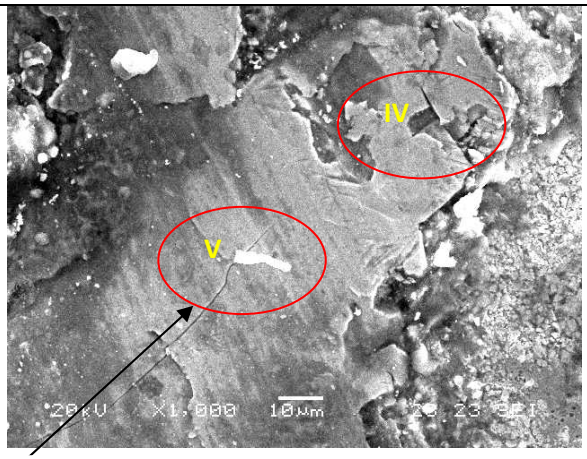

Figure 4c: 5%Ni composite of 40N Contact Load

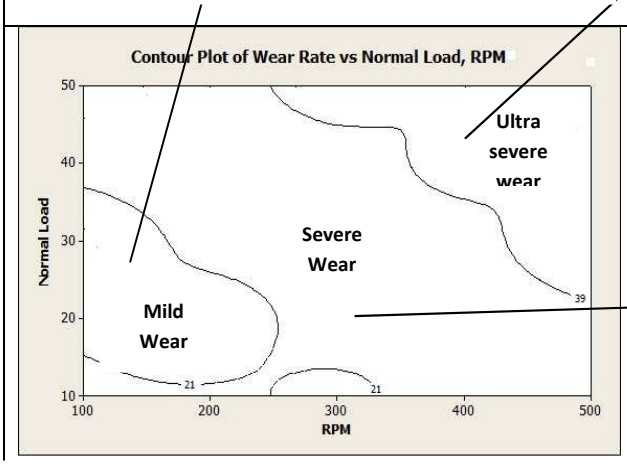

Figure 4a: Wear Transition Map

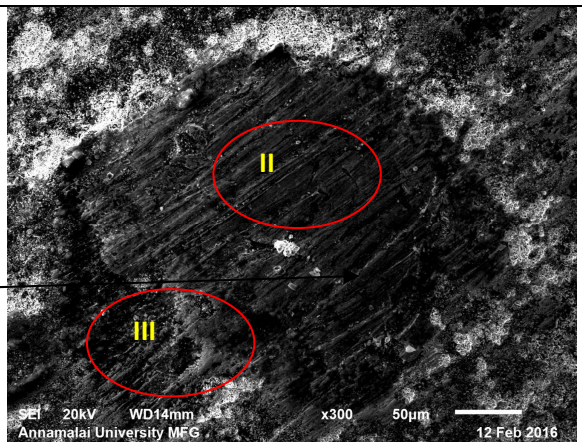

Figure 4b: 5%Ni composite of 30N Contact Load

I. Ironing, II. Scratching, III. Ploughing, IV. Plastic Deformation, V. Fatigue Wear

Figure 4: Wear Mechanism Map WC-5%Ni Composite

It is observed that the SEM micro graph results are well correlating with the results of graphical representation.

The wear mechanisms can be classified into two groups ; one is abrasive wear and other is adhesive wear. The ploughing and scratching falls under the category of abrasive whereas the plastic deformation and fatigue wear comes under the category of adhesive wear [21].

Wear mechanism map indicates the locations of the dominance of five different wear mechanisms and is shown in Figure.4. Using Mini tab 16 software and the observations on the worn out surfaces, wear mechanism maps are constructed. The different field boundaries on the map suggest where transitions of one dominant wear mechanism to another may take place. The physical wear mechanism maps need extensive physical modeling for determination of boundaries for different mechanisms.

In empirical maps, the boundaries are constructed roughly based on the observations of the worm out surface. Mini tab 16 is comparatively scientific in construction of field boundaries on SEM observations [21]. Because of the wide range of sliding velocity and contact pressure covered by the map, it should enable the designer to decide intelligently whether the material under study will be able to meet the set of requirements for a particular tribological application.

CONCLUSIONS

- The state of ceramic wear is briefly recognized by mild wear, severe wear and ultra-sever wear from the viewpoints of wear surface roughness and wear rate.
- From the nature of contour maps, the occurrence of a wear transition can be easily identified on the contour maps as the lines of contact wear rates bunch together to represent a steep ascent.
- The line boundaries that can be plotted to show the locations where the transition occur. There may be one or several transitions with in the speed and load ranges studied in this work, it is usually a mild to severe wear transition and transition from severe wear to ultra-severe wear. The locations of these wear transition zones for a given material pair vary within the different speed and different load ranges
- The wear rate increases with increasing binder content, this is as expected since the greater volume fraction of Ni results in a greater fraction of the easily removable binder phase which will allow undermining of particles to take place more easily and subsequently result in a higher rate of particle pullout.

REFERENCES

1. *Aristizabal, M., Rodriguez, N., Ibarreta, F., Martinez, R., & Sanche, Z. (2010). Liquid phase sintering and oxidation resistance of WC–Ni–Co–Cr cemented carbides. International Journal of Refractory Metals & Hard Materials, 28(4), 516-522.*
2. *Ahmadian, M., Wexler, D., Chandra, T., & Calka, A. (2005). Abrasive wear of WC–FeAl–B and WC–Ni3Al–B composites. International Journal of Refractory Metals & Hard Materials, 23(3), 155-159.*
3. *Pandey, P. C., & Jilani, S. T. (1987). Electrical machining characteristics of cemented carbides. Wear, 116, 77-88.*
4. *Cornelissen, H. R., Snoeys, & Kruth, J. P. (1977). Investigation on the optimal machining conditions for electro-discharge machining of cemented carbides. Transactions of NAMRI/SME, 5, 258-264.*
5. *Lee, S. H., & Li, X. P. (2001). Study of the effect of machining parameters on the machining characteristics in electrical discharge machining of tungsten carbide. Journal of Materials Processing Technology, 115, 344-358.*
6. *Qu, Jun, Laura, R., Albert J. S., Ronald O. S., Edgar L. C., & Thomas R. W. (2003). Nano indentation characterization of*

surface layers of electrical discharge machined WC–Co. Materials Science and Engineering A, 344, 125-131.

7. *Myers Raymond, H., & Montgomery, D. C. (2002). Response Surface Methodology: process and product optimization using designed experiment. A Wiley-Interscience Publication. ISBN: 978-0-470-17446-3.*
8. *Becher, P. F., & Plucknett, K. P. (1997). Properties of Ni_3Al-bonded titanium carbide ceramics. Journal of the Eurpean Ceramic Society, 18, 395-400.*
9. *Chen, J. L., Zhu Ding, Y., & Lin Deng, Y. (2006). Advances in Ni_3Al-based alloys research and application. Materials Review, 20(1), 35-38.*
10. *Tumanov, A. V., Gostev, Y. V., Panov, V. S., & Kots, Y. F. (1986). Wetting of TiC−WC system carbides with molten Ni3Al. Soviet Powders Metall Metal Ceram, 25(5), 428-430.*
11. *Tiegs, T. N., Alexander, K. B., Plucknett, K. P., Menchhofer, P. A., Becher, P. F., & Water, S. B. (1996). Ceramic composites with a ductile Ni_3Al binder phase. Materials Science and Engineering A, 209(1−2), 243-247.*
12. *Williams, J. A. (1999). Wear modeling analytical, computational and mapping a continuum mechanics approach. Wear, 229, 1-17.*
13. *Van Acker, K. (2005). Influence of tungsten carbide particle size and distribution on the wear resistance of laser clad WC/Ni coatings. Wear, 258, 194–202.*
14. *Garcai, I., Fransaer, J., Celis, J. P. (2001). Electrode opostion and sliding wear resistance of Ni-composite coatings containing micron and submicron SiC particles. Surf Coat Tech, 148,171–178.*
15. *Priit Podra, & Soren Andersson, (1997). Simulating sliding wear with finite element method. Journal of Tribology International, 32, 71–81.*
16. *Srinivasan, V., Karthikeyan, R., Mohamad Raffi, N., & Ganesan, G. (2010). Wear Characteristics of Nano-Particle Filled GFRP Composites. Advanced Composites Letters, 19, 1-10.*
17. *Samyn, P., De Bacts, P., Schoukens, G., & Quintelier, J. (2007). Wear transitions and stability of poly oxy methylene homo polymer in highly loaded applications compared to small scale testing. Tribology International, 40, 819-833.*
18. *Koji, K., & Koshi, A. (2002). Wear of advanced ceramics. Wear, 253, 1097–1104.*
19. *Beste, U., Hammer, S. I., Engqvist, H., Rimlinger, S., & Jacopson, S. (2001). Particle erosion of cemented carbide with low Co content. Wear, 250, 809-817.*
20. *Adachi, K., Kato, K., Chen, N. (1997). Wear map of ceramics. Wear, 203, 291-301.*
21. *Lim, S. C. (1998). Recent developments in wear mechanism maps. Journal of Tribology International, 31,87-97.*